

Motor Modelling and Magnetic adhesion Simulation For Hybrid Wall Climbing AGV

Lokesh Ramesh

Department of Mechatronics Engineering,
School of Mechanical Sciences,
Hindustan Institute of Technology and
Science, Chennai, Tamil Nadu, India.
Lokesh2000227@gmail.com

Crispin Marie Peter G

Department of Mechatronics Engineering,
School of Mechanical Sciences,
Hindustan Institute of Technology and
Science, Chennai, Tamil Nadu, India.
vineethcrispin@gmail.com

Gladwyn K

Department of Mechatronics Engineering,
School of Mechanical Sciences,
Hindustan Institute of Technology and
Science, Chennai, Tamil Nadu, India.
gladymdu@gmail.com

Sundeep R

Department of Mechatronics Engineering,
School of Mechanical Sciences,
Hindustan Institute of Technology and
Science, Chennai, Tamil Nadu, India.
Sundeeps242002@gmail.com

Tharun A

Department of Mechatronics Engineering,
School of Mechanical Sciences,
Hindustan Institute of Technology and
Science, Chennai, Tamil Nadu, India.
tharunkumar270402@gmail.com

Ramkumar

Department of Mechatronics Engineering,
School of Mechanical Sciences,
Hindustan Institute of Technology and
Science, Chennai, Tamil Nadu, India.
dinakaran@hindustanuniv.ac.in

Abstract— The AGV's are beginning to change the way of the industries, there are still rooms for development of those AGV's. The hybrid AGV's which can climb walls and move on land for various purposes. The magnetic adhesion plays a major role in deciding the payload of the robot. The distance between the magnet and the iron rail surface embedded in the wall. The analysis was done on the magnet and the metal surface with FEMM software to find the best position to place the magnet in the robot. The distance between the magnet and the iron rail was also analyzed to reduce the friction and avoid magnets sticking to the rail. As it was found that the magnets positioning does play an important role in the overall payload and to give the required data to design the AVG to increase its performance. The design of the AGV is an important factor to consider the payload and the balance of the robot while climbing the wall to make sure that it doesn't fail. The motor modelling has been done with the help of MATLAB and the results are been recorded and is used for further studies and to incorporate the same in the mechanical design and make the AGV work properly. In summarizing the work, the magnets along with a design can improve the overall ability to perform the operations is essential, also the Motor modelling and the analysis done in MATLAB with Simulink will provide the results and data to make the AGV move with more precision.

Keywords—AGV, Hybrid AGV, Wall Climbing Robot, Magnetic Wall Climbing robot.

I. INTRODUCTION

Wall climbing robots generally use different methods to climb wall. One of the most efficient ways is to use magnetic adhesion method. This method is used in ferric materials to make the bot climb the walls where it is hazardous to man to reach or it could be a task which has to be repeated for n number of times which could be tiresome for men. These AGVs makes the work easier for them by automating it. These hybrid AGVs can both climb walls as well as move on land. The magnets are placed on one side of the robot which will provide the required adhesion force for the robot to climb the wall and carry the load placed on it. The magnetic adhesion force acts as a gravity on

another direction, making the robot to stick in two axis and provide motion in the third.

These move like the caterpillar or any worm which secretes its own fluid to stick on to the wall and crawl on them even though they carry their food along with them. These are known to be biomimicry where we learn, the way nature works and mimic them to aid mankind in ways that we want. There are different ways for different species of animals to climb walls. One used here is similar to a worm crawling on the wall. The rails are provided here to guide the robot to move in the certain direction along the rails and help to achieve the destination.

II. MATERIAL AND DESIGN ANALYSIS OF MAGNET AND YOKE

A. Magnets and CAD model

There are different grades of neodymium magnets ranging from N30 to N52, where the grade goes up as the power of the magnets go up. The magnets are placed in a yoke with equal intervals. The magnets are tested against a ferric material that is been embedded against the wall for the robot to climb. Block magnets are used as they are easy to mount in the yoke. The dimension of the magnet is 50x50x25. And the block magnets are fragile so they require a yoke to be placed in.

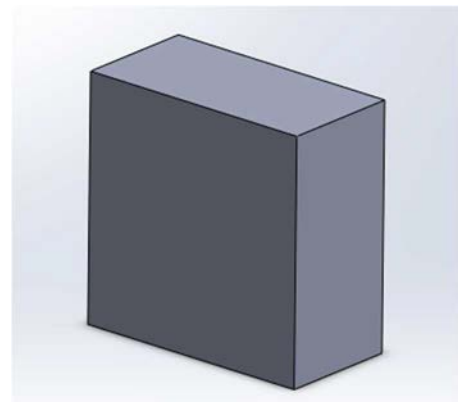


Fig 1. CAD model of the magnet.

The magnets are placed in the yoke. The yoke is made up of a low carbon steel where it is milled and the slots for magnet are milled out perfectly to fit in 2 magnets with equal interval and with correct thickness. The magnets placed next to each are made sure that they are of opposite polarity so that the strength of the magnet improves and the adhesion force is increased.

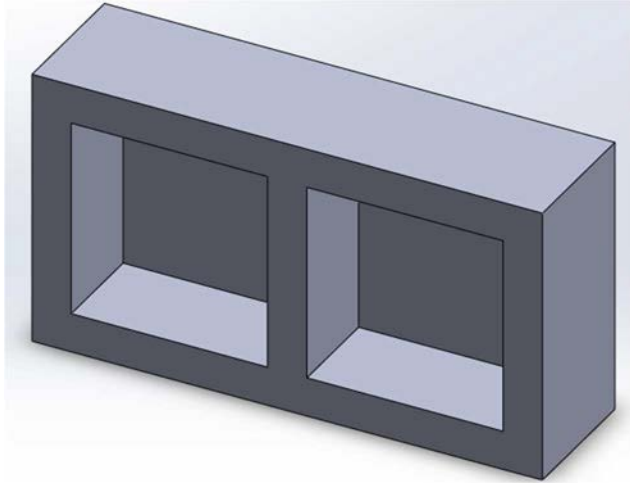


Fig 2. Yoke

The magnets are secured in this yoke and are mounted on the AGV. The analysis of the magnet is been done in FEMM software.

III. MAGNETIC ANALYSIS ON FEMM SOFTWARE

The FEMM v4.2 software is used to calculate the adhesion generated by the magnets. This software tool is used to perform finite element simulations, thereby approximating adhesion under various scenarios. The magneto statics problem encompasses this type of issue. Pre-processing, processing, and post-processing are the three steps that must be taken in this software to solve the problem. The initial processes involve modelling the required geometry with the FEMM's pre-processor tools. The first step is to specify the problem as magneto statics and to define the depth. These tools include nodes, lines, and arcs that can be used to build the model. The next step involves specifying the material by manually entering the properties or selecting from FEMM's built-in library. After the materials are specified in the drawn model, an enclosure is built around it to make the problem to be solved a finite one. The following step is to convert this continuous problem into a discrete problem. This is known as meshing, and it is done automatically by FEMM. Running the FEM and viewing the results are the next inline processes. This task has been completed using post-processing tools. The materials for N52 magnets and their values are specified in the Built-In library of the FEMM software.

The thickness of the Metal plate is 8MM and the magnets are placed in different distances to analyze the magnetic adhesion force exerted between the magnets in the yoke to the metal plate.

It is tested for various distances and the data is been recorded and tabulated. Then the required distance is been selected. Then the yoke is been mounted so that the clearance is maintained between the magnets and the yoke.

A. Analysis On Magnets N52 and N35

For knowing the difference in the strength of the magnets the comparative study has been made similar to the earlier study between N35 and N52.

Table I Comparing N35 and N52

S. No	Analysis On N35 and N52		
	Gap between plate and Magnet	N52	N35
1	2MM	26902.7 N	20745.3 N
2	5MM	15551.1 N	11633 N
2	7MM	12039.3 n	8905.52 N
4	10MM	8731.6 N	6387.02 N
5	12MM	2588.2 N	1892.89

B. Analysis on N52 magnets with differenct clearance:

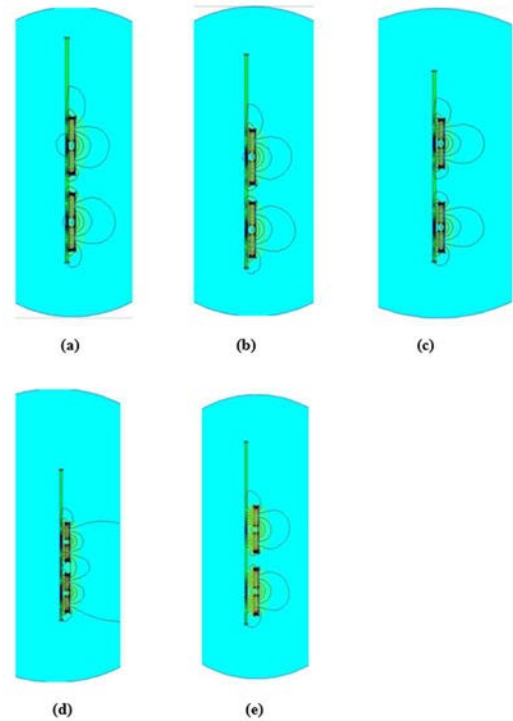


Fig 3. FEMM analysis

The FEMM analysis done in different spacing is shown here and the field strength is been shown to know the strength of the adhesion force of the magnets.

Table II N52 Analysis

No.	Gap between plate and Magnet	N52
a	2MM	26902.7 N

No.	Gap between plate and Magnet	N52
b	5MM	15551.1 N
c	7MM	12039.3 n
d	10MM	8731.6 N
e	12MM	2588.2 N

The table is the result of the analysis done in FEMM. The distance between the plate and the magnets and the magnetic adhesion force in newtons is given in this table. This analysis proves to be useful in calculating the payload of the robot. Now that this is confirmed the pay load can be decided on the basis of the load that we need to carry on the wall. Here the selected distance is 12 mm and that distance proves to be safe when mounted. In that distance the payload is being satisfied. Even if the payload has to be increased the yoke can be adjusted and kept closer to carry more load.

IV. MATHEMATICAL MODELLING OF DC MOTOR

A. Speed Equation

ω = Angular velocity can also be used as $\dot{\theta}$
as $\omega = \dot{\theta}$

$$\omega = V * K_v$$

so,

$$V = 1/K_v * \omega$$

As,

$$1/K_v = K_e \quad \text{--1}$$

Therefore,

$$V_e = K_e * \omega \quad \text{--2}$$

(V_e = back emf generated)

$$\omega = V_e / K_e \quad \text{--3}$$

Torque equation:

As voltage is directly proportional to speed, the current is directly proportional to Torque.

$$T = K_t * I \quad \text{--4}$$

(T is the torque and K_t is torque constant)

These 1,2 and 4 equations represent that K_e, K_v and K_t are linked together. They can be equated with a few steps.

According to KVL,

$$V_{in} = I.R + V_e$$

$$V_{in} = I.R + K_e * \omega \quad \text{--5}$$

(sub from (2))

Now using this in power equation,

$$P_{in} = (I.R + K_e * \omega) I \quad \text{--6}$$

(sub from (5))

$$I^2.R + I.K_e * \omega$$

As mechanical power out = torque X rotational speed,
Mechanical power out = $T * \omega$

$$\text{Mechanical power out} = I * K_t * \omega \quad \text{--7}$$

(sub from (4))

Losses in the circuit,

$$\text{Losses} = I^2.R$$

Equating Electrical power in to Mechanical power out and adding losses i.e., losses + (7) = (5),

$$I^2.R + I.K_e * \omega = I^2.R + I.K_t * \omega$$

Which leaves,

$$K_e = K_t \quad \text{--8}$$

As to remove the proportionality symbol the torque constant K_t is been introduced. These equations show the relationship between voltage, speed and backemf.

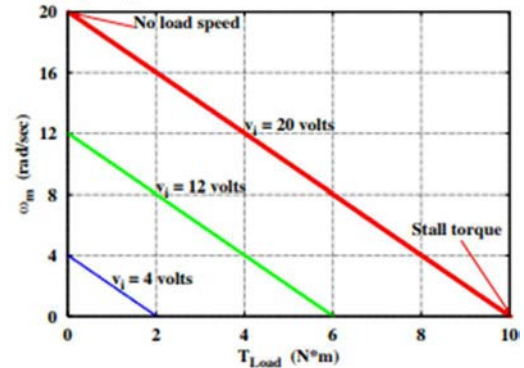


Fig 4. speed torque graph

This graph shows the speed load and torque variations. The speed increases and load decreases. This shows that the current drawn is less for less load the voltage remains constant as the rated voltage is. The increase in load causes more current and when the load increases after the rated load the motor stops rotating and the current drawn is at its peak. This condition is known as the stall torque.

Considering these factors, the motor has been selected and is been tested in this equation to find the constants present and solved in MATLAB.

B. Motor Model

Mechanical model:

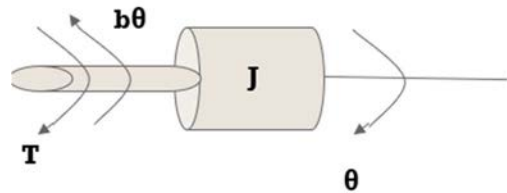


Fig 5. Mechanical Model of a motor

$$T_m = K_t I = T_l + J \frac{d\omega}{dt} + b \frac{d\omega}{dt}$$

Taking Laplace Transform,

$$T_m(s) = T_l(s) + JS \omega(s) + B \omega(s)$$

$$\omega(s) = (T_m(s) - T_l(s)) / (J s + B) \quad -- 9$$

$$\begin{aligned} V(s) &= R i(s) + L s i(s) + K \omega(s) \\ I(s) &= (V(s) - K \omega(s)) / (R + L s) \quad -- 10 \end{aligned}$$

Electrical Model:

Here

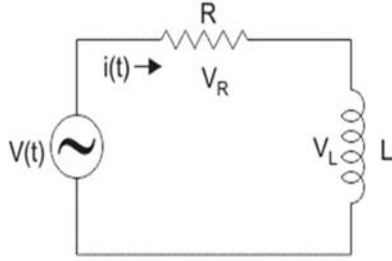


Fig 6. Electrical model of a motor

$$V - R i - L \frac{di}{dt} - V_{emf} = 0$$

(according to KVL)

$$V - R i - L \frac{di}{dt} - K_e \omega = 0$$

(as $V_{emf} = K_e \cdot d\theta/dt$, $\omega = d\theta/dt$)

Taking Laplace transform,

Solving 4 and 5 will give the final motor equation as done in MATLAB.

V. MATLAB MODELLING AND SIMULATION

The Simulink model was designed on the basis of the Motor modelling where the constants are given their respective values that have been derived by calculations and solving various equations separately and been applied here. These values have been verified using the real time model and has been simulated to get the resulting graph. The dead weight and payload have been distinguished here. The Dead weight is been subtracted from the payload and is calculated in the overall load capability of the AGV. The value of torque when the AGV is running without any loads applied is noted. When there is any deviation in the torque of the motor i.e., the current consumption of the motor increases and the speed fluctuates. That can be the sign that an external load is been applied on the AGV. The increase in the current settles at a point indicating the load is constant.

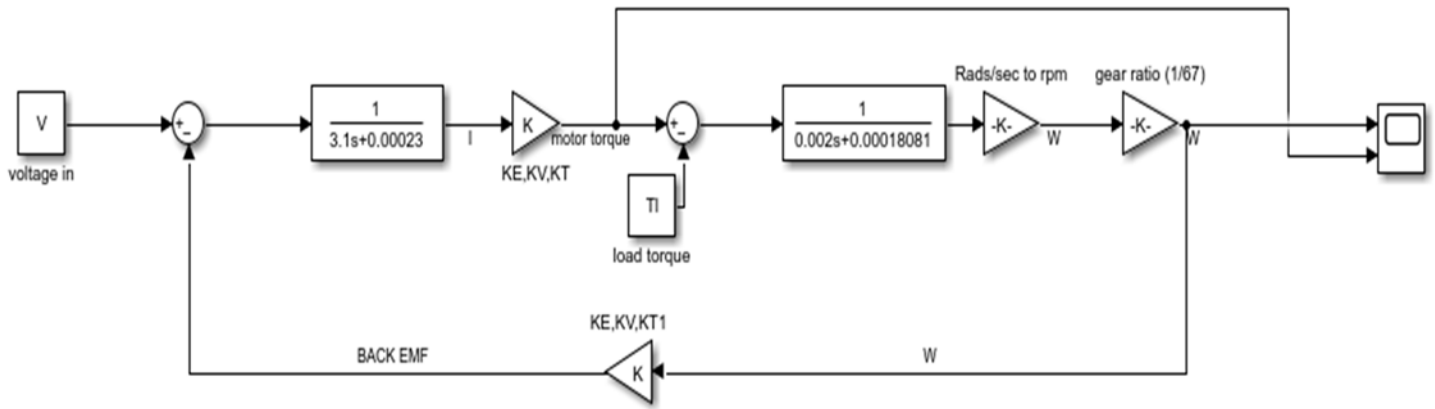


Fig 7. Simulink Model

The Output of the simulation is torque and speed. As the tests prove when the load is increased the speed of the motor reduces. In order to compensate with that PID controller has been chosen to be used and compute the speed and maintain the speed in the suitable conditions of the motor i.e., working under the rated conditions of the motor. The output may be uncertain if the load applied is more than that of what this motor can handle. The load value is been used within the range of the motor and been simulated. The V i.e., voltage is the given input and the out is the torque and the speed of the motor been measured and seen through scope. As the load increases the speed decreases and that is been given to the P controller to maintain the speed of the motor. As mentioned only P controller is being used as the study on PID has been done that has been mentioned as well. The outputs of the P controller is being used from each motor to operate in a manner where the main controller gets those data and make it run smoother.

VI.FINAL MODEL

The full mathematical model is going to contain the same motor equation 4 times and is been given to a separate controller for each motor to have its own control algorithm to control the motor. A master board will be present to give the control signals to the slave boards to control the operation.

I2C protocol is been used for communication. This protocol requires only 2 wires to send data from one device to another. This protocol can be used to connect up to 112 devices. There are 2 wires namely SDA and SCL. SDA means serial data and SCL means serial clock. These two lines send the data. Clock Pulse is mainly used for reading or writing or to send acknowledge bit and to transfer the data faster.

The data can be transferred up to 10 khz. This method is used here and each slave has its own address so the master will address the slave with its corresponding address before

sending the data. The slave receives and processes the data to control the speed of the motor. The speed control is done with PID controller which is widely used to control the speed of the motor. This control algorithm requires feedback from the motor. The feedback is from the encoder and that data is been read by each controller and the speed is computed.

There is a set speed given to the controller. This checks if the difference between the set speed and the current speed is zero. If yes then it continues to help the motor maintain the same speed. If no then the controller sends the difference between the two to the controller and increases the Voltage to match the required speed

There are 3 parameters in the PID controller. P stands for proportional; I stand for integral and, D stands for Derivative. In this we have only used P to control the motor as that is sufficient to control the speed and is stable enough to work in these situations.

The general PID block diagram explains the working of the PID controller. That is implemented in the final modelling and added to the control system.

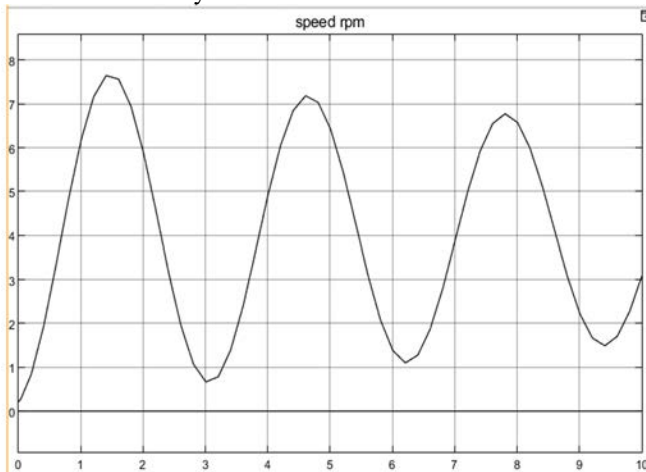


Fig 8. Speed of the motor from the model.

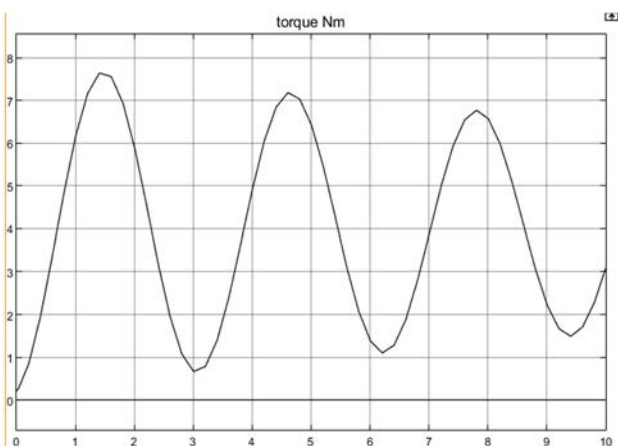


Fig 9. Torque of the Motor from the Model

VII. RESULTS OF SIMULINK

The result is the graph of torque (N/M) and speed in RPM the output is a sine wave where the voltage is been continuously

varied. As the graph represents the speed is less where the torque is higher and the torque is less where the speed is higher. The motor modelling along with the PID is used to make the full model of the motor.

This model has to be used along with 4 motors and is synchronized to make the AGV run. The PID algorithm will make use of the feedback from the Encoders to get the speed of the motor continuously and maintain the speed of the motor. The concept of Master-Slave is been used where one controller acts as master giving the rest of the controllers the data to process the speed on. Conclusion and Future work

The research concludes that the Magnetic adhesion simulation proved to be useful in selection of the magnets and in the placement of the magnet in the vehicle. The mathematical modelling simulation and analysis has been a major guidance in selecting the right motor that has to be used in the AGV. The load analysis for payload and dead load and making them differentiate was much clear to make the robot stable and will be much easier to implement the same in the PID controller. As mentioned, the PID that is used here is not fully developed and only the part of the work that has been done has been described here. the method to differentiate the dead load and pay load will be implemented at the earliest.

Magnets that are used for carrying materials in construction sites. The future work includes the building of the structure, then creating a controller to control this robot effectively and run this on land and on walls. This can be improved and create various versions and can be used in construction sites. This has a lot of unexplored areas where this reduces the work of humans and incorporate robots to make the work faster and more accurate. A system of centralized Control can be built and various wall climbing AGVs with their purposes like carrying loads and pouring cement, and for wiring in the constructed building can be implemented and the construction blue print and the plan can be programmed in the central system and the AGVs and bots added to it are compatible where they automatically get the works assigned and the progress of the whole project can be seen in the central system's display.

ACKNOWLEDGMENT

This work is been supported by the department of Mechatronics, Hindustan institute of technology and science under ANRO which has been supporting all new engineers to develop new bots for the future.

REFERENCES

- [1] Nansai, S. and Mohan, R.E., 2016. A survey of wall climbing robots: recent advances and challenges. *Robotics*, 5(3), p.14.
- [2] Jose, J., Dinakaran, D., Ramya, M.M., Kuppan Chetty, R.M., Tokhi, M.O. and Sattar, T.P., 2020. Investigations on the effect of wall thickness on magnetic adhesion for wall climbing robots. *International Journal of Robotics and Automation*. DOI: 10.2316/J.2021.206-0441
- [3] Jose, J., Elankavi, R.S., Dinakaran, D., Chetty, R.K. and Ramya, M.M., 2020, December. Optimization of Distance Between Magnets for Magnetic Wall Climbing Robots. In 2020 3rd International Conference on Intelligent Sustainable Systems (ICISS) (pp. 1574-1578). IEEE.

- [4] Saif Sabah Sami¹, Zeyad Assi Obaid², Mazin T. Muhssin³, Ali N. Hussain⁴, Jun 2021. Detailed modelling and simulation of different DC motor types for research and educational purposes. DOI: 10.11591/ijpeds.v12.i2.pp703-714.
- [5] Samir Metha and John Chiasson, "Nonlinear Control of a Series DC Motor: Theory and Experiment". IEEE Transactions on Industrial Electronics, Vol.45, No. 1, 1998.
- [6] Jesús U. Liceaga-Castro, Irma I. Siller-Alcalá, Jorge Jaimes-Ponce & Roberto Alcántara-Ramírez, 2017. Series DC Motor Modeling and Identification. In International Conference on Control, Artificial Intelligence, Robotics & Optimization. DOI:10.1109/ICCAIRO.2017.54
- [7] J. Jose, R. S. Elankavi, D. Dinakaran, R. K. Chetty and M. M. Ramya, "Optimization of Distance Between Magnets for Magnetic Wall Climbing Robots," 2020 3rd International Conference on Intelligent Sustainable Systems (ICISS), 2020, pp. 1574-1578, doi: 10.1109/ICISS49785.2020.9315911.
- [8] F. Ochoa-Cardenas and T. J. Dodd, "Design of an active magnetic wheel with a varying Electro-Permanent Magnet adhesion mechanism," 2015 IEEE/RSJ International Conference on Intelligent Robots and Systems (IROS), 2015, pp. 3340-3345, doi: 10.1109/IROS.2015.7353842.
- [9] A. S. Semenov, V. M. Khubieva and Y. S. Kharitonov, "Mathematical Modeling of Static and Dynamic Modes DC Motors in Software Package MATLAB," 2018 International Russian Automation Conference (RusAutoCon), 2018, pp. 1-5, doi: 10.1109/RUSAUTOCON.2018.8501666.
- [10] B. Fecko and A. Kalinov, "Matlab Model and PI Controller of DC Permanent Magnet Motor," 2019 IEEE International Conference on Modern Electrical and Energy Systems (MEES), 2019, pp. 370-373, doi: 10.1109/MEES.2019.8896578.
- [11] Junxi Cai, Chunyan Lai and N. C. Kar, "Modeling and analysis of torque ripple in a brushless DC motor considering spatial harmonics," 2017 IEEE 30th Canadian Conference on Electrical and Computer Engineering (CCECE), 2017, pp. 1-4, doi: 10.1109/CCECE.2017.7946709.
- [12] Z. Zakaria, M. S. B. Mansor, A. H. Jahidin, M. S. Z. Azlan and R. A. Rahim, "Simulation of magnetic flux leakage (MFL) analysis using FEMM software," 2010 IEEE Symposium on Industrial Electronics and Applications (ISIEA), 2010, pp. 481-486, doi: 10.1109/ISIEA.2010.5679417.
- [13] P. Grmela, M. Mach and V. Hájek, "Permanent magnet DC motor re-design by FEMM," International Aegean Conference on Electrical Machines and Power Electronics and Electromotion, Joint Conference, 2011, pp. 666-669, doi: 10.1109/ACEMP.2011.6490679.
- [14] H. S. Hameed, "Brushless DC motor controller design using MATLAB applications," 2018 1st International Scientific Conference of Engineering Sciences - 3rd Scientific Conference of Engineering Science (ISCES), 2018, pp. 44-49, doi: 10.1109/ISCES.2018.8340526.
- [15] Virgala, Ivan, Peter Frankovský, and Mária Kenderová. "Friction effect analysis of a DC motor." American Journal of Mechanical Engineering 1.1 (2013): 1-5.
- [16] Danielle collins